



Higher visible photocatalytic activities of nitrogen doped In_2TiO_5 sensitized by carbon nitride

Yuan Liu, Gang Chen*, Chao Zhou, Yidong Hu, Dingguo Fu, Jie Liu, Qun Wang

Department of Chemistry, Harbin Institute of Technology, Harbin 150001, PR China

ARTICLE INFO

Article history:

Received 19 September 2010
Received in revised form 26 February 2011
Accepted 28 February 2011
Available online 4 March 2011

Keywords:

Photocatalytic activity
Visible light
N-doped In_2TiO_5
Carbon nitride

ABSTRACT

N-doped In_2TiO_5 modified by carbon nitride (CN) composite (NICN) has been prepared by the pyrogenation of the mixture of urea and In_2TiO_5 through a polymerizable complex (PC) method. The powder samples were characterized by XRD, FESEM, TEM, UV–vis, and XPS. It is shown by XRD that the precursor sintered at 1000 °C is pure and nitrogen dopant does not change the crystal structure of In_2TiO_5 . FESEM and TEM reveal a hole-like morphology of the prepared NICN. With the increase of nitrogen content, the light absorption onset of In_2TiO_5 shifts from 410 nm to 450 nm, revealing significant narrowing of the band gap. XPS results suggest that only 2.2% of the nitrogen atoms were doped into In_2TiO_5 through the urea pyrogenation method. Furthermore, the decomposition of Rhodamine B (Rh-B) under visible light reveals that Rh-B can be degraded completely within 20 min and recycling experiments indicate NICN has stable structure and durable photocatalytic activity, suggesting a promising utilization of such photocatalyst under visible light. Finally, an innovative mechanism of N-doped In_2TiO_5 sensitized by carbon nitride polymer is proposed.

© 2011 Elsevier B.V. All rights reserved.

1. Introduction

Global crisis of energy and environment has been issues for decades. Among the various solutions, semiconductor particles used as photocatalysts to decompose water polluted by organic and for hydrogen evolution have been explored by scientists since titania was first described as a catalyst for photochemical water splitting [1]. So far, titanate-based photocatalysts have been achieved such as BaTiO_3 [2], MnTiO_3 [3], CdTiO_3 [4], CaTiO_3 [5] and In_2TiO_5 [6]. Some of them display good photocatalytic activity and chemical stability. However, most of them are limited for use under UV-light. While the content of UV-light in the sunlight spectral is less than 5%, and in contrast, visible light whose wavelength ranges from 420 to 750 nm accounts for 43%. To take the best advantage of solar light, exploring catalysts with visible light photocatalytic activity is necessary and significant.

The crystal structure of In_2TiO_5 is a three-dimensional tunneling structure, built by octahedral InO_6 and TiO_6 [6]. UV–vis diffuse reflectance spectroscopy indicates that its energy band gap is 3.02 eV. Recently, In_2TiO_5 has received much attention due to its reasonable activities for the decomposition of organic pollutants and the split of water under UV irradiation. The In_2TiO_5 synthesized by Wang et al. [6] through sol–gel revealed better photocatalytic

activity than TiO_2 (P25) in degrading Methyl Orange. Shah et al. [7] synthesized V-doped In_2TiO_5 , which showed both UV-light and visible light activity. In recent study, nonmetal adulteration can stimulate the absorption peak to shift to long wavelength zone, making the catalysts possess visible light activity, and thus the utilization of sunlight is enhanced. N-doped photocatalyst is a focus of study in photocatalytic field. So far, N- TiO_2 [8], N- SrTiO_3 [9,10], N-doped titanate nanotubes [11], N- $\text{H}_2\text{Ta}_2\text{O}_6$ [12], N- NaTaO_3 [13] and N- NaNbO_3 [14], all display good visible light activities. However, to the best of our knowledge, there are few investigations concerning the effects of In_2TiO_5 doped with nonmetal element on the photocatalytic activity.

Yan et al. reported that graphite C_3N_4 photocatalyst possessed good environmental adaptability, which can be directly applied to industrial wastewater treatment to degrade organic pollutants [15]. Besides, because of its unique surface and electronic structure, carbon nitride is an attractive material for potential applications such as hydrogen production [16–19] and electrochemically catalyzes oxygen reduction [20]. Furthermore, Mitoraj et al. [21] and Yang et al. [22] reported that not only nitrogen was doped into the photocatalyst but also some carbon nitride polymers were composited on the surface of the photocatalyst.

Herein, a novel N-doped In_2TiO_5 sensitized by carbon nitride was synthesized by heating the mixture of urea and the precursor In_2TiO_5 at 400 °C for 2 h. The photocatalytic activity of NICN was evaluated by decomposing Rh-B aqueous solution under visible light. Rh-B, as one important represent of xanthene dyes, is

* Corresponding author. Fax: +86 451 86413753.
E-mail address: gchen@hit.edu.cn (G. Chen).

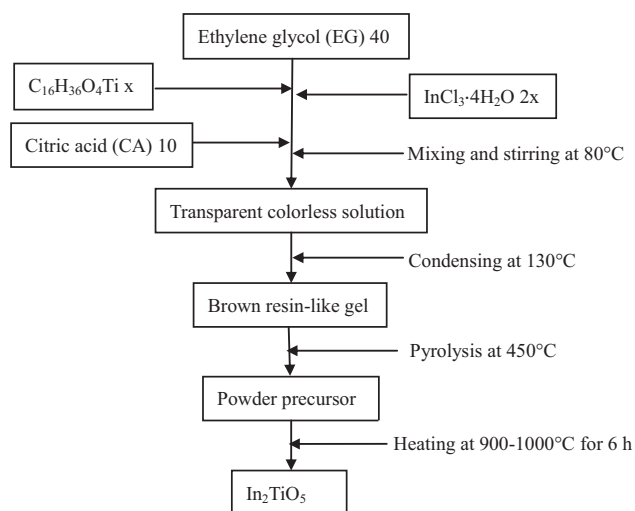


Fig. 1. Flowchart for the polymerizable complex procedure used to prepare powders.

famous for its good stability as dye laser materials, which is also a kind of common organic pollutant, and photodegradation of Rh-B is important with regard to the purification of dye effluents [23]. In order to investigate the stability and durable activity of NICN, the recycling experiments were also carried out.

2. Experimental methods

2.1. Synthesis of photocatalyst

In_2TiO_5 powders were firstly synthesized by PC method as outlined in Fig. 1 [24]. $\text{C}_{16}\text{H}_{36}\text{O}_4\text{Ti}$ and $\text{InCl}_3 \cdot 4\text{H}_2\text{O}$ were chosen as metal sources. Ethylene glycol (EG) was used as the solvent and anhydrous citric acid (CA) was used as a chelating agent to stabilize In and Ti ions. CA was first dissolved in EG, followed by adding $\text{C}_{16}\text{H}_{36}\text{O}_4\text{Ti}$ and $\text{InCl}_3 \cdot 4\text{H}_2\text{O}$ with continuous stirring at 80°C until the solution became transparent and colorless. Then the solution was heated at 130°C to promote polymerization between CA and EG, during which it became more viscous and finally a brown resin-like gel was obtained 12 h later. The brown gel was heated at 450°C for several hours to burn out unnecessary organics, followed by calcination at 1000°C for 6 h in air to produce the precursor. The precursor powder was mixed with urea completely, which was then heated at 400°C for 2 h to produce NICN. All chemical agents were obtained from Shanghai Reagent Co., China.

2.2. Catalyst characterization

The crystal structures of the obtained materials were confirmed by a powder X-ray diffractometer (XRD, Rigaku D/max-2000) with monochromated Cu $K\alpha$ radiation (45 kV, 50 mA). The scanned range was $2\theta = 10\text{--}90^\circ$, with speed of $5^\circ/\text{min}$. Ultraviolet–visible (UV–vis) diffuse reflection spectra were measured for the catalysts using a UV–vis spectrometer with an integrating sphere (PG, TU-1900/1901). The XPS spectra were collected on an American Electronics physical PHI5700ESCA system X-ray photoelectron spectroscopy using Al $K\alpha$ radiation (1486.6 eV). The source was operated at 12.5 kV and the anode power was 250 W. The binding energy (BE) was calibrated with the C 1s peak. Morphologies were observed by field-emission scanning electron microscopy (FESEM, MX2600FESEM) and transmission electron microscopy (TEM, FEI, Tecnai G2 S-Twin).

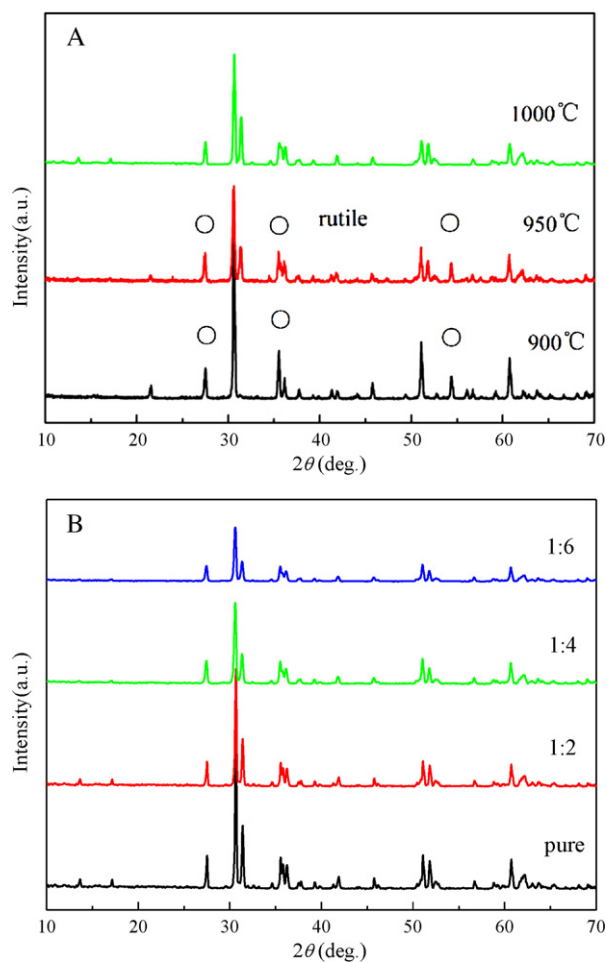


Fig. 2. (A) XRD patterns of In_2TiO_5 sintered at different temperatures and (B) NICN sintered with various ratios of In_2TiO_5 to urea.

2.3. Photoactivity test

The photocatalytic activities of NICN were tested by the degradation of Rh-B under visible light irradiation. A 300 W Xe lamp with a cut-off filter (400 nm) was used as the light source. 0.2 g catalyst powder was dissolved in aqueous solution of Rh-B (100 mL, 10 mg/L) in vessel. The pH value of the reaction suspension was adjusted by adding different amounts of HCl solution. Prior to irradiation, the suspensions were first ultrasonicated for 10 min, and then magnetically stirred in dark for 50 min to achieve adsorption and desorption equilibrium. During the Rh-B photodecomposition, 3 mL of aliquots were collected with syringe in every given time interval. The photocatalyst and the Rh-B solution were separated from each filtrate sample by a centrifuge at 10,000 rpm for 10 min. The filtrates were analyzed by UV–vis spectrometer with an integrating sphere (PG, TU-1900/1901).

3. Results and discussion

3.1. X-ray diffraction analysis

The crystalline phase of In_2TiO_5 and NICN was analyzed by X-ray diffraction. Fig. 2A shows XRD patterns of In_2TiO_5 synthesized at different calcination temperatures for 6 h. Obviously, the calcination temperature has great influence on the formation of In_2TiO_5 crystalloids. At 900°C , the diffraction peaks indicate the characteristic of In_2O_3 and TiO_2 , which means that the reaction between In_2O_3 and TiO_2 did not take place at all. At 950°C , there are still

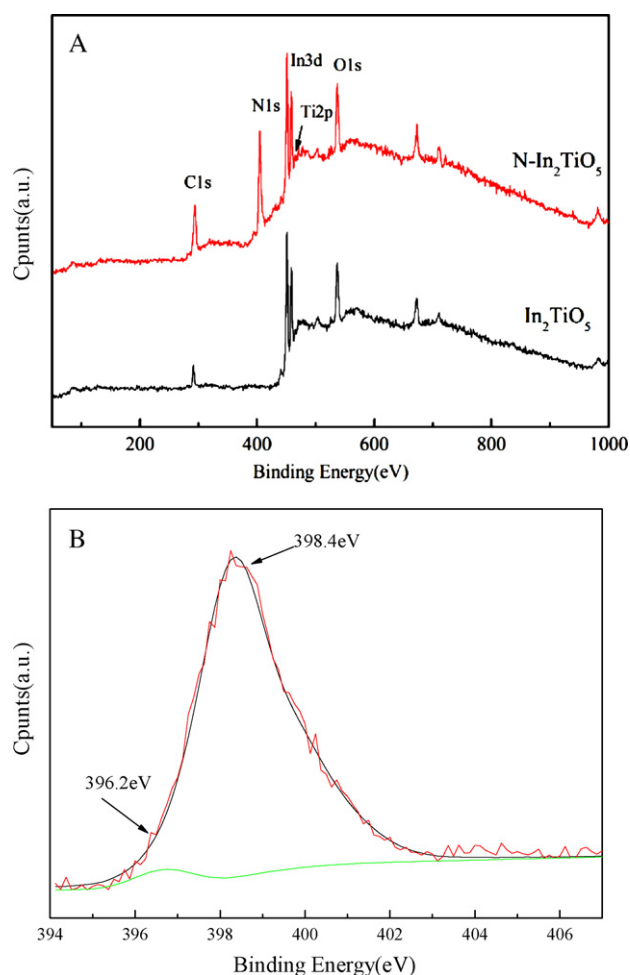


Fig. 3. XPS spectra of pure In_2TiO_5 and NICN.

some diffraction peaks of In_2O_3 and TiO_2 . However, when the calcination temperature was increased to 1000°C the diffraction peaks show good agreement with those in the standard card (PDF 30-0640), namely, the pure phase In_2TiO_5 was synthesized at 1000°C .

To investigate the effect of the N content on the crystal structure, the XRD experiments of NICN calcinated with various mass ratios of In_2TiO_5 to urea were carried out in this paper. As shown in Fig. 2B, although the intensity of diffraction peaks decreased with the increase of nitrogen content, the diffraction characteristic of NICN is very similar with that of pure phase In_2TiO_5 . In other words, N dopant has little effect on the crystal structure of In_2TiO_5 .

3.2. XPS analysis

Considering that N content has little effect on the crystal structure of In_2TiO_5 , X-ray photoelectron spectroscopy technique was employed to confirm whether nitrogen was doped into In_2TiO_5 . TEM picture in Fig. 4C shows that the surface of In_2TiO_5 is covered by some materials. Fig. 3A is the XPS spectra of pure In_2TiO_5 and $\text{N-In}_2\text{TiO}_5$. After urea treatment, the intensity of N 1s peak and the C 1s peak increased, indicating that the surface of In_2TiO_5 is covered by the polymers containing CN bonds. Similar phenomenon was also reported by Li et al. [12]. The N 1s peaks of NICN between 394 and 407 eV were deconvoluted by the Gaussian function into two peaks centered at 396.2 eV and 398.4 eV as shown in Fig. 3B. The peak at 396.2 eV arose from Ti–N [25–27] is assigned as atomic $\beta\text{-N}$ which had great bearing on the photocatalytic activity, and the peak at 398.4 eV, corresponding to C–N bond, is assigned as molec-

Table 1
Band gap energy varies with different mass ratios between urea and In_2TiO_5 .

Urea/ In_2TiO_5 (mass ratio)	Band gap (eV)
0	3.02
2	2.95
4	2.86
6	2.75

ularly chemisorbed $\gamma\text{-N}$ [28,29]. The density of N from Ti–N in the powder samples was evaluated to be 2.2 at.%, therefore only a small amount of nitrogen is doped into In_2TiO_5 . Similar phenomena about nitrogen dopant were also found in other reports [10,30].

3.3. Morphology of the photocatalysts

The morphologies of In_2TiO_5 and NICN were characterized by FESEM. As shown in Fig. 4B, carbon nitride has significant effect on the microscopic morphologies of In_2TiO_5 compared with Fig. 4A. After adulteration, particles show high porosity owing to the carbon nitride which may have bearing on photocatalytic activity. Nevertheless, it is invalid to acknowledge that carbon nitride polymer covered the surface of In_2TiO_5 only from the SEM images. To further investigate the fine morphology of NICN, the TEM image is shown in Fig. 4C. Plus the XPS result above that the intensity of N 1s and C 1s signals increased, clearly, the surface of In_2TiO_5 is surrounded by the nanoporous CN polymers.

3.4. UV–vis diffuse reflectance property

To study the optical absorption properties of the samples, UV–vis diffuse reflectance spectra of In_2TiO_5 and NICN synthesized with different nitrogen content are displayed in Fig. 5. It can be seen that the absorption edge of pure phase In_2TiO_5 is 410 nm and the absorption edge shifts to long wavelength range with the increase of the nitrogen content. Finally, the absorption edge reaches 450 nm when the mass ratio of In_2TiO_5 to urea is 1:6. According to the equation $E_g = 1240/\lambda_g$ (nm), the band gap energy values for different samples are calculated and summarized in Table 1. With the increase of mass ratio of urea to In_2TiO_5 , the band gap energy is reduced to 2.75 eV from 3.02 eV, indicating that the obtained samples have obvious absorption in visible light region.

3.5. Photocatalytic degradation of Rh-B

The photocatalytic activity of NICN was evaluated by decomposing Rh-B under visible light irradiation ($\lambda > 400$ nm). To investigate the absorption ability of nanoglued particles, the degradation of Rh-B solution was run under dark condition which is graphically illustrated in Fig. 6A. It can be seen that the nanoglued samples have weak absorption ability from the dark line. According to the red line in Fig. 6A, when there is no catalyst, the absorbency of original Rh-B solution exhibits almost no difference from the absorbency of Rh-B when they are illuminated under visible light from a 300 W Xenon lamp for 20 min. So we can conclude that the Rh-B is stable in the experimental conditions. In order to study the influence of nitrogen content, samples prepared with different mass ratios of In_2TiO_5 to urea were used to decompose Rh-B (100 mL, 10 mg/L). The results in Fig. 6A show that NICN has optimal photocatalytic activity when the mass ratio is 1:6 which is in agreement with UV–vis diffuse reflectance spectra.

3.6. Effects of acid

The effect of acid on photocatalytic activity of NICN (mass ratio = 1:6) was also studied. Adjust the pH value of Rh-B (100 mL,

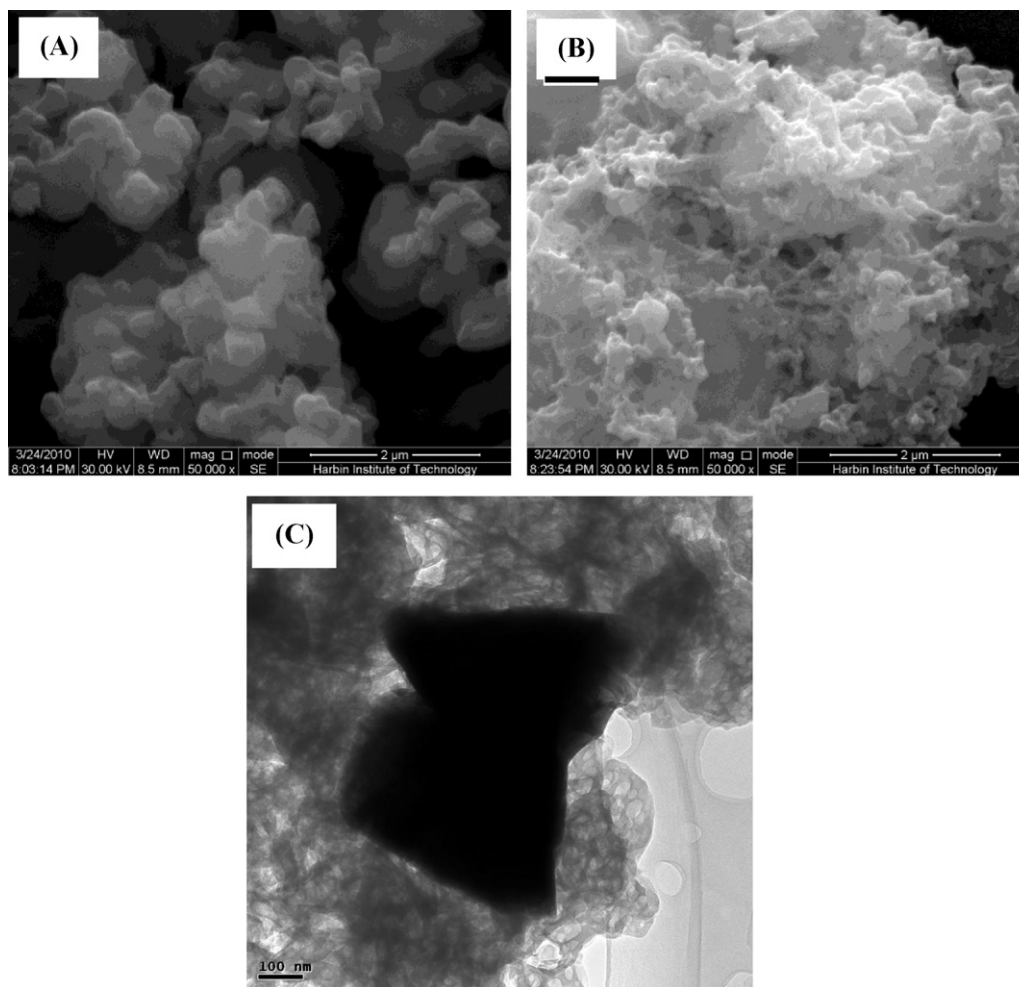


Fig. 4. FESEM images of pure In_2TiO_5 (A) and NICN (B) sintered at 1000°C , TEM image of NICN (C) sintered at 1000°C .

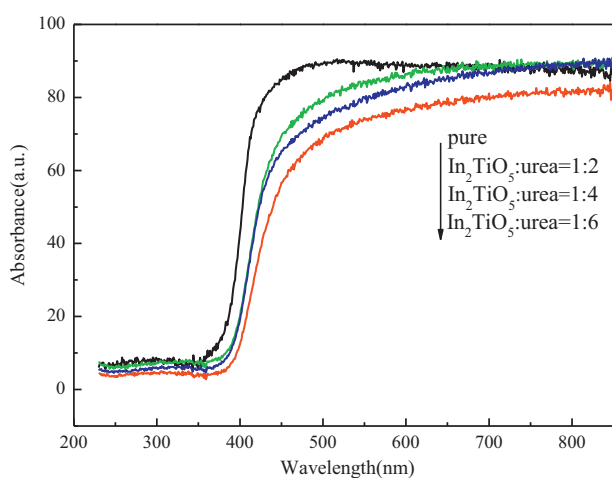


Fig. 5. UV-vis diffuse reflectance spectra of original In_2TiO_5 and NICN with different mass ratios.

10 mg/L) to pH = 1, pH = 3, pH = 5, pH = 7 by adding 1000 μL , 10 μL , 0.1 μL , 0 μL HCl (10.00 M/L), respectively. The results of decomposition are shown in Fig. 6B, and it can be seen that NICN (mass ratio = 1:6) has the best degradation rate and the complete degradation of Rh-B was achieved in less than 20 min when pH = 1. The photocatalytic activity of NICN strongly depends on pH value. The increase of pH is conducive to the dissociation of Rh-B at $-\text{COOH}$

sites, thus hinders it to diffuse into the bubble–liquid interface, where uncombined $\cdot\text{OH}$ concentration is maximum [31,32], therefore the decolorization rate of Rh-B is decreased. We all know that O_2 is a main factor for organic pollutants photodegradation and affects the formation of superoxide ($\text{O}_2\cdot^-$) via direct reduction of O_2 and hydroxyl radicals ($\cdot\text{OH}$) via multistep reduction of O_2 :



Both photogenerated holes and hydroxyl radicals can directly react with organic pollutants. So the increase of the H^+ density can further indirectly make NICN produce more hydroxyl radicals and more holes (reactions (2) and (3)) [15]. In addition, the protonic acidity of HCl could make NICN hydrate more easily in aqueous solutions of Rh-B and then favor the electron transfer between NICN and H^+ (H_2O) species [33,34].

3.7. Reusability of NICN

Durable photocatalytic activity and reusable stability are significant to any photocatalysts. Subsequently, the recycling experiments on NICN (mass ratio = 1:6) were also carried out under the same reaction conditions. The catalysts were separated from the reaction mixture by centrifugation after each reaction cycle.

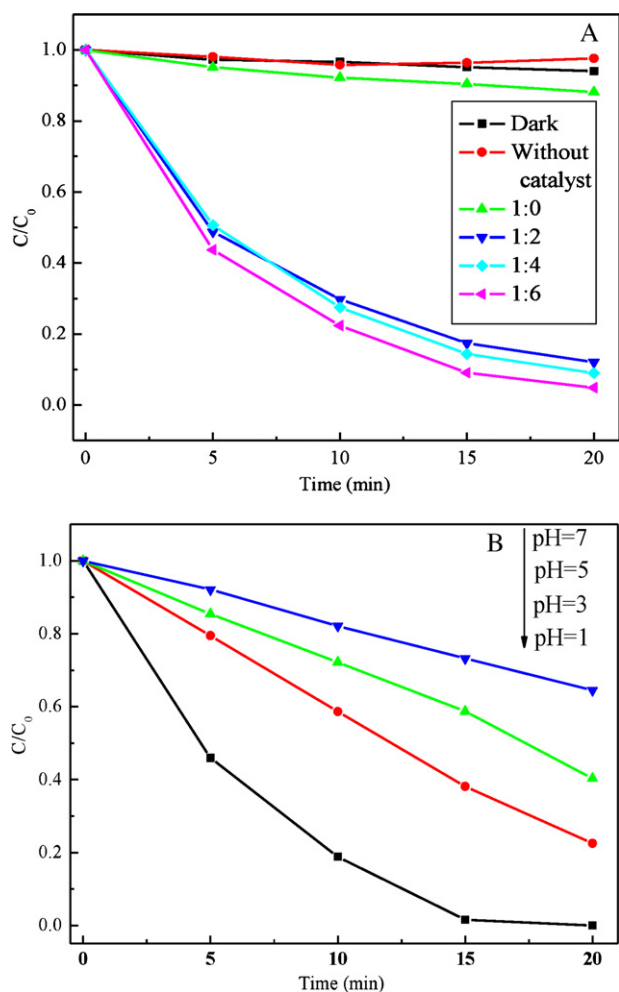


Fig. 6. (A) The black line denotes the absorption ability of catalyst in dark condition; the red line denotes the influence of visible light on Rh-B without catalysts; the rest denote the influence of different N dopant content on the decomposition rate of Rh-B; (B) the influence of acid concentration on the decomposition rate of Rh-B. (For interpretation of the references to color in this figure caption, the reader is referred to the web version of the article.)

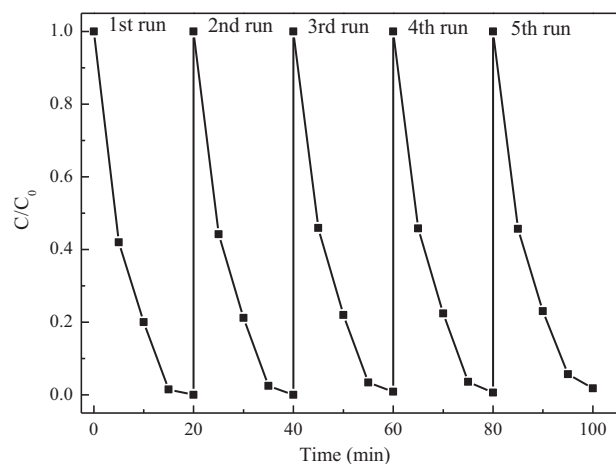


Fig. 7. Reusable stability of NICN (mass ratio = 1:6) under the same condition.

After the Rh-B photodegradation reaction was repeated five times, the results in Fig. 7 indicate that the NICN possesses high durable photocatalytic activity and reusable stability during the recycling process.

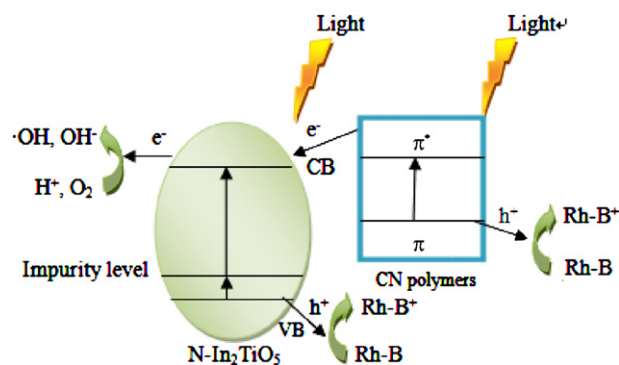


Fig. 8. Proposal of the photocatalytic reaction mechanism of Rh-B decomposition on nitrogen doped In_2TiO_5 sensitized by CN polymers.

3.8. Mechanism of nitrogen doped In_2TiO_5 sensitized by carbon nitride

To some extent, high visible photocatalytic activity can be attributed to the increase of the separation rate of photoinduced electron–hole pairs, because CN polymers which covered the surface of In_2TiO_5 could transfer the excited electrons [17]. In addition, when the mass ratio of In_2TiO_5 to urea reached 1:6, catalysts can harness more visible light according to UV–vis diffuse reflectance spectra because of its higher light absorption onset. Also, it is entirely possible that the high porosity in Fig. 4B may provide more reaction sites for catalysts to decompose Rh-B.

However, we think that the reaction mechanism plays the most significant role to improve the catalysts' visible light photocatalytic activity. As shown in Fig. 8, when the photocatalysts are irradiated by the visible light, the excited electrons on the valance band can be transferred to conduction band via impurity level which is begot by nitrogen dopant. Then, holes are induced on valance band and electrons are accumulated on conduction band. The holes oxidant directly react with Rh-B on condition that the pH value is lower than 3 rather than react with H_2O (OH^-) and form $\cdot\text{OH}$ which will further decompose Rh-B [35]. On the other hand, the electrons on the HOMO (high occupied molecular orbital) level of the CN polymers are excited to jump to the LUMO (low unoccupied molecular orbital) level and then transfer to the conduction band of the nitrogen dopant In_2TiO_5 . So the holes on the HOMO level of the CN polymers will hardly recombine with excited electrons but react with Rh-B directly [12]. As a result, the nitrogen doped In_2TiO_5 is sensitized by CN polymer and NICN has a higher visible light photocatalytic activity.

4. Conclusion

In summary, NICN catalysts have been successfully prepared through a polymerizable complex method. The decomposition of Rh-B indicates that NICN (mass ratio = 1:6) displays the highest visual light photocatalytic activity, and Rh-B (100 mL, 10 mg/L) was degraded completely in less than 20 min. The nanoporous CN polymers have great effect on the photocatalytic activity which is in agreement with other reports. Moreover the recycling experiments indicate that NICN has commendably durable photocatalytic activity and reusable stability. The successful modification of In_2TiO_5 through nitrogen dopant will provide some valuable instruction for other photocatalysis materials. The potential application of metal and nitrogen coadulteration and carbon nitride composite materials to organic compounds decomposition and hydrogen production could be studied in the future.

Acknowledgements

The authors gratefully thank the National Nature Science Foundation of China (Project Nos. 20871036 and 21071036) and National Innovative Experiment Program for Undergraduate.

References

- [1] A. Fujishima, K. Honda, Electrochemical photolysis of water at a semiconductor electrode, *Nature* 238 (1972) 37–38.
- [2] D. Zhao, D. Ying, C. Wen, X.M. Pei, Synthesis and characterization of single-crystalline BaTi_2O_5 nanowires, *J. Phys. Chem. C* 114 (2010) 1748–1751.
- [3] Z.Q. Song, S.B. Wang, W. Yang, W.M. Li, H. Wang, Y. Hui, Synthesis of manganese titanate MnTiO_3 powders by a sol–gel–hydrothermal method, *Mater. Sci. Eng. B* 113 (2004) 121–124.
- [4] H. Wang, X.X. Zhang, A.P. Huang, H.Y. Xua, M.K. Zhu, B. Wang, H. Yan, M. Yoshimurab, A new phase of cadmium titanate by hydrothermal method, *J. Cryst. Growth* 246 (2002) 150–154.
- [5] L.S. Cavalcante, V.S. Marques, J.C. Sczancoski, M.T. Escotec, M.R. Joy, J.A. Varela, M.R.M.C. Santos, P.S. Pizani, E. Longo, Synthesis, structural refinement and optical behavior of CaTiO_3 powders: a comparative study of processing in different furnaces, *Chem. Eng. J.* 143 (2008) 299–307.
- [6] W.D. Wang, F.Q. Huang, C.M. Liu, X.P. Lin, J.L. Shi, Preparation, electronic structure and photocatalytic activity of the In_2TiO_5 photocatalyst, *Mater. Sci. Eng. B* 139 (2007) 74–80.
- [7] P. Shah, D.S. Bhang, A.S. Deshpande, M.S. Kulkarnib, N.M. Gupta, Doping-induced microstructural, textural and optical properties of $\text{In}_2\text{Ti}_{1-x}\text{V}_x\text{O}_{5+\delta}$ semiconductors and their role in the photocatalytic splitting of water, *Mater. Chem. Phys.* 117 (2009) 399–407.
- [8] Y.Q. Wang, X.J. Yu, D.Z. Sun, Synthesis, characterization, and photocatalytic activity of TiO_2-xN_x nanocatalyst, *J. Hazard. Mater.* 144 (2007) 328–333.
- [9] J.S. Wang, S. Yin, K. Masakazu, Q.W. Zhang, S. Fumio, S. Tsugio, Photo-oxidation properties of nitrogen doped SrTiO_3 made by mechanical activation, *Appl. Catal. B: Environ.* 52 (2004) 11–21.
- [10] J.S. Wang, S. Yin, K. Masakazu, Q.W. Zhang, S. Fumio, S. Tsugio, Preparation and characterization of nitrogen doped SrTiO_3 photocatalyst, *J. Photochem. Photobiol. A: Chem.* 165 (2004) 149–156.
- [11] Y.P. Peng, S.L. Lo, H.H. Ou, S.W. Lai, Microwave-assisted hydrothermal synthesis of N-doped titanate nanotubes for visible-light-responsive photocatalysis, *J. Hazard. Mater.* 183 (2010) 754–758.
- [12] Q.Y. Li, B. Yue, I. Hideo, K. Tetsuya, J.H. Ye, Carbon nitride polymers sensitized with N-doped tantalum acid for visible light-induced photocatalytic hydrogen evolution, *J. Phys. Chem. C* 114 (2010) 4100–4105.
- [13] D.R. Liu, C.D. Wei, B. Xue, X.G. Zhang, Y.S.J. Jiang, Synthesis and photocatalytic activity of N-doped NaTaO_3 compounds calcined at low temperature, *J. Hazard. Mater.* 182 (2008) 50–54.
- [14] H.F. Shi, X.K. Li, Hideo, Z.G. Zou, J.H. Ye, 2-Propanol photodegradation over nitrogen-doped NaNbO_3 powders under visible-light irradiation, *J. Phys. Chem. Solids* 70 (2009) 931–935.
- [15] S.C. Yan, Z.S. Li, Z.G. Zou, Photodegradation of Rhodamine B and Methyl Orange over boron-doped $\text{g-C}_3\text{N}_4$ under visible light irradiation, *Langmuir* 26 (2010) 3894–3901.
- [16] X.C. Wang, M. Kazuhiko, X.F. Chen, T. Kazuhiro, K. Domen, Y. Hou, X.Z. Fu, M. Antonietti, Polymer semiconductors for artificial photosynthesis: hydrogen evolution by mesoporous graphitic carbon nitride with visible light, *J. Am. Chem. Soc.* 131 (2009) 1680–1681.
- [17] X.F. Chen, Y.S. Jun, K. Takanahe, K. Maeda, K. Domen, X.Z. Fu, M. Antonietti, X.C. Wang, Ordered mesoporous SBA-15 type graphitic carbon nitride: a semiconductor host structure for photocatalytic hydrogen evolution with visible light, *Chem. Mater.* 21 (2009) 4093–4095.
- [18] J. Zhang, X. Chen, K. Takanahe, K. Maeda, K. Domen, J.D. Epping, X. Fu, M. Antonietti, X. Wang, Synthesis of a carbon nitride structure for visible-light catalysis by copolymerization, *Angew. Chem. Int. Edit.* 122 (2010) 451–454.
- [19] X. Wang, K. Maeda, A. Thomas, K. Takanahe, G. Xin, J.M. Carlsson, K. Domen, M. Antonietti, A metal-free polymeric photocatalyst for hydrogen production from water under visible light, *Nat. Mater.* 8 (2009) 76–80.
- [20] M. Stephen Lyth, Y. Nabae, S. Moriya, S. Kuroki, M. Kakimoto, J. Ozaki, S. Miyata, Carbon nitride as a nonprecious catalyst for electrochemical oxygen reduction, *J. Phys. Chem. C* 113 (2009) 20148–20151.
- [21] D. Mitoraj, H. Kisch, The nature of nitrogen-modified titanium dioxide photocatalysts active in visible light, *Angew. Chem. Int. Edit.* 47 (2008) 9975–9978.
- [22] G.Q. Li, N. Yang, W.L. Wang, W.F. Zhang, Synthesis, photophysical and photocatalytic properties of N-doped sodium niobate sensitized by carbon nitride, *J. Phys. Chem. C* 113 (2009) 14829–14833.
- [23] M. Asiltürk, F. Sayılkan, S. Erdemoğlu, M. Akarsu, H. Sayılkan, M. Erdemoğlu, E. Arpaç, Characterization of the hydrothermally synthesized nano- TiO_2 crystallite and the photocatalytic degradation of Rhodamine B, *J. Hazard. Mater.* 129 (2006) 164–170.
- [24] M. Yoshino, M. Kakihana, W.S. Cho, H. Kato, A. Kudo, Polymerizable complex synthesis of pure $\text{Sr}_2\text{Nb}_x\text{Ta}_{2-x}\text{O}_7$ solid solutions with high photocatalytic activities for water decomposition into H_2 and O_2 , *Chem. Mater.* 14 (2002) 3369–3376.
- [25] J. Yuan, M.X. Chen, J.W. Shi, W.F. Shangguan, Preparations and photocatalytic hydrogen evolution of N-doped TiO_2 from urea and titanium tetrachloride, *Int. J. Hydrogen Energy* 31 (2006) 1326–1331.
- [26] H. Irie, Y. Watanabe, K. Hashimoto, Nitrogen-concentration dependence on photocatalytic activity of TiO_2-xN_x powders, *J. Phys. Chem. B* 107 (2003) 5483–5486.
- [27] P. Romero-Gómez, V. Rico, A. Borrás, A. Barranco, J.P. Espinós, J. Cotrino, A.R. González-Elipse, Chemical state of nitrogen and visible surface and schottky barrier driven photoactivities of N-doped TiO_2 thin films, *J. Phys. Chem. C* 113 (2009) 13341–13351.
- [28] R. Asahi, T. Morikawa, T. Ohwaki, Visible-light photocatalysis in nitrogen-doped titanium oxides, *Science* 293 (2001) 269–271.
- [29] S.F. Chen, X.Q. Liu, Y.Z. Liu, G.Y. Cao, The preparation of nitrogen-doped TiO_2-xN_x photocatalyst coated on hollow glass microbeads, *Appl. Surf. Sci.* 253 (2007) 3077–3082.
- [30] D.J. Pulsipher, I.T. Martin, E.R. Fisher, Controlled nitrogen doping and film colorimetrics in porous TiO_2 materials using plasma processing, *Appl. Mater. Inter.* 2 (2010) 1743–1753.
- [31] R. Kidak, N.H. Ince, Effects of operating parameters on sonochemical decomposition of phenol, *J. Hazard. Mater.* B137 (2006) 1453–1457.
- [32] M.A. Behnajady, N. Modirshahla, S. Bavili Tabrizi, S. Molanee, Ultrasonic degradation of Rhodamine B in aqueous solution: influence of operational parameters, *J. Hazard. Mater.* 152 (2008) 381–386.
- [33] X. Li, N. Kikugawa, J. Ye, Nitrogen-doped lamellar niobic acid with visible light-responsive photocatalytic activity, *Adv. Mater.* 20 (2008) 3816–3819.
- [34] X. Li, N. Kikugawa, J. Ye, A comparison study of rhodamine B photodegradation over nitrogen-doped lamellar niobic acid and titanic acid under visible-light irradiation, *Chem. Eur. J.* 15 (2009) 3538–3545.
- [35] Y. Sun, J.J. Pignatello, Evidence for a surface dual hole-radical mechanism in the TiO_2 photocatalytic oxidation of 2,4-dichlorophenoxyacetic acid, *Environ. Sci. Technol.* 29 (1995) 2065–2072.